THE JOURNAL OF COMPARATIVE NEUROLOGY 494:651–662 (2006)

AII Amacrine Cells in the Distal Inner Nuclear Layer of the Mouse Retina

EUN-JIN LEE,[1] LAURA B. MANN,[1] DENNIS W. RICKMAN,[2] EUN-JIN LIM,[3] MYUNG-HOON CHUN,[3] AND NORBERTO M. GRZYWACZ[1]*
[1]Department of Biomedical Engineering, Neuroscience Graduate Program, and Center for Vision Science and Technology, University of Southern California, Los Angeles, California 90089-1111
[2]Departments of Ophthalmology and Neurobiology, Duke University, Durham, North Carolina 27710
[3]Department of Anatomy, College of Medicine, The Catholic University of Korea, 137-701 Seoul, Korea

ABSTRACT

We serendipitously found a distal Disabled-1 (Dab1)-immunoreactive cell in retina of the C57BL/6J black mouse. The somata of these cells are located in the outermost part of the inner nuclear layer (INL). Their processes extend toward the outer plexiform layer (OPL), receiving synaptic inputs from horizontal and interplexiform cells. In the current study, we name this cell the "distal Dab1-immunoreactive cell." Double-labeling experiments demonstrate that the distal Dab1-immunoreactive cell is not a horizontal cell. Rather, the distal Dab1 cell appears to be a misplaced AII cell, by being glycine transporter-1-immunoreactive and by resembling the latter cell in an electron microscopic analysis. A distal Dab1 cell had been reported in the FVB/N mouse retina, a model of retinitis pigmentosa (Park et al. [2004] Cell Tissue Res 315:407–412). However, here, we found this distal Dab1-immunoreactive cell in the adult and normal developing mouse retinas. Hence, we show that such cells do not require the loss of photoreceptors as suggested previously (Park et al. [2004] Cell Tissue Res 315:407–412). Instead, two other pieces of data suggest an alternative explanation sources for distal Dab1 cells. First, we find a correlation between the number of these cells in the left and right eyes Second, developmental analysis shows that the distal Dab1-immunoreactive cell is first observed shortly after birth. At the same time, AII cells emerge, extending their neurites into the inner retina. These data suggest that distal Dab1-immunoreactive cells are misplaced AII amacrine cells, resulting from genetically modulated anomalies owing to migration errors. J. Comp. Neurol. 494:651–662, 2006.

Indexing terms: Disabled-1; AII amacrine cells; glycine transporter-1; calbindin; horizontal cells; immunocytochemistry

Disabled-1 (Dab1) is a critical component of the reelin signaling pathway that controls the laminar organization of brain structures, such as the cerebellum, cerebral cortex, and hippocampus (for review see Rice and Curran, 1999). Dab1 encodes a cytoplasmic protein containing a motif known as a protein-interaction/phosphotyrosine-binding domain. This domain was originally identified in the adaptor protein, shc, as a region required for binding to the epidermal growth factor receptor and other tyrosine-phosphorylated proteins (Margolis, 1996). In the mammalian central nervous system, tyrosine phosphorylation of Dab1 promotes its interaction with several non-receptor tyrosine kinases, including Src, Fyn, and Ab1. The interaction between Dab1 and these kinases is through their SH2 domains. Howell et al. (1997) reported that Dab1 functions in kinase-signaling cascades during development, and Dab1 plays an important role in the final positioning of migrating neurons.

Grant sponsor: National Eye Institute; Grant number: EY08921 (to N.M.G.); Grant number: EY11170 (to N.M.G.); Grant sponsor: Research to Prevent Blindness (to D.W.R.); Grant sponsor: Neurobiology Research Center; Grant number: M10412000009-05N1200-00910 (to M.-H.C.).

*Correspondence to: Norberto M. Grzywacz, Department of Biomedical Engineering, University of Southern California, Denney Research Building 140, Los Angeles, CA 90089-1111. E-mail: nmg@bmsr.usc.edu

Received 5 April 2005; Revised 29 July 2005; Accepted 8 September 2005
DOI 10.1002/cne.20838
Published online in Wiley InterScience (www.interscience.wiley.com).

TABLE 1. List of Antibodies Applied

Antiserum	Immunogen	Source	Working dilution
Rabbit polyclonal anti-Disabled-1 (Dab1)	Peptide C-terminal: CGEPPSGGDNISPQDGS that corresponds to the mDab555 sequence beginning at residues 542–558	Dr. B. Howell, NIH (Howell *et al.*, 1997).	1:1,000
Mouse monoclonal anticalbindin	Purified bovine kidney calbindin D-28k	Sigma, St. Louis, MO (C9848)	1:6,000
Goat polyclonal antiglycine transporter-1 (GLYT1)	Synthetic peptide corresponding to the carboxy-terminus as predicted from the cloned rat GLYT1	Chemicon International, Temecula, CA (AB1770)	1:10,000
Mouse monoclonal antipostsynaptic density protein (PSD)	Purified recombinant rat PSD-95	Affinity Bioreagents, Golden, CO (MA1-046) (clone 7E3-1B8)	1:500
Mouse monoclonal antiglutamate decarboxylase 65 (GAD65)	Human GAD65 from baculovirus-infected cells	Chemicon International, Temecula, CA (MAB351)	1:500

Recently, antiserum against Dab1 has been shown to label a specific class of retinal amacrine cell, the AII. These cells have narrow-field, bistratified processes that arborize in sublaminae a and b of the retinal inner plexiform layer (IPL; Rice and Curran, 2000; Lee et al., 2003, 2004). They are important interneurons of the rod pathway, being interposed between rod bipolar cells and ON and OFF cone bipolar cells (Kolb and Famiglietti, 1974; McGuire et al., 1984; Strettoi et al., 1992; Chun et al., 1993). Rice and Curran (2000) showed that Dab1 plays a role in the segregation of functionally distinct synapses in the IPL during development of the mouse retina. They also suggested that the expression of Dab1 by AII amacrine cells allows them to be positioned properly in response to reelin, produced by adjacent ganglion cells.

However, in mouse retina, not all AII amacrine cells seem to be positioned properly. In the present study, we describe a distal Dab1 glycinergic cell in the adult and developing retinas of the C57BL/6J black mouse. This cell was not described in a previous paper by Rice and Curran (2000). However, a similar cell in the outer part of the INL has been reported for the FVB/N mouse retina (Park et al., 2004). Because that retina is a model for retinitis pigmentosa, the authors suggested that the distal Dab1 cells were due to photoreceptor loss. In contrast, the retinas studied here are normal, so photoreceptor loss cannot explain our results. Finally, we report on the synaptic connectivity of this distal Dab1-immunoreactive cell. A partial description of the distal Dab 1 cell appeared previously in abstract form (Grzywacz et al., 2005).

MATERIALS AND METHODS

Tissue preparation

Five litters of C57BL/6J black mouse were used for Dab1 studies at diverse developmental stages [postnatal (P) days 1, 3, 5, 7, 10, 15, and 21, and adult mice]. All procedures with mice were in conformance with the *Guide for care and use of laboratory animals* (National Institutes of Health). These procedures were approved by the University of Southern California Institutional Animal Care and Use Committee. The animals were deeply anesthetized by intraperitoneal injection of pentobarbital (40 mg/kg body weight), and the eyes were enucleated. The anterior segments were then removed, and the eyecups were fixed by immersion in 4% paraformaldehyde in 0.1 M phosphate buffer (PB), pH 7.4, for 2–3 hours. After fixation, retinas were carefully dissected and transferred to 30% sucrose in PB for 24 hours at 4°C. Retinas were then frozen in liquid nitrogen, thawed, and rinsed in 0.01 M phosphate-buffered saline (PBS; pH 7.4).

Immunocytochemistry

For fluorescence Dab1 immunocytochemistry, 50-μm-thick vibratome sections were incubated in 10% normal goat serum (NGS) and 1% Triton X-100 in PBS for 1 hour at room temperature. This incubation was to block nonspecific binding sites. Sections were then incubated overnight with a rabbit polyclonal antibody directed against Dab1. This Dab1 antibody (kindly provided by Dr. B. Howell, NIH) was developed in rabbit with the peptide C-terminal CGEPPSGGDNISPQDGS. This terminal corresponds to the mDab555 sequence beginning at residues 542–558 (Howell et al., 1997). The antiserum was used at a dilution of 1:1,000 in PBS containing 0.5% Triton X-100 at 4°C. Retinas were washed in PBS for 45 minutes (3 × 15 minutes). Afterward, we incubated retinas for 2 hours in carboxymethylindocyanine (Cy3)-conjugated affinity-purified, donkey anti-rabbit IgG (1:500 dilution; Jackson Immunoresearch, West Grove, PA) at room temperature. Retinal sections were washed for 30 minutes with 0.1 M PB and coverslipped with 10% glycerol in 0.1 M PB. For retinal whole-mount immunostaining, the same immunocytochemical procedures described above were used, but with longer incubation times [3 days in Dab1 and 2 days in (Cy3)-conjugated affinity-purified, donkey anti-rabbit IgG with the same dilution as described above]. Immunofluorescence images were imported into Adobe Photoshop 7.0 (Adobe Systems, Mountain View, CA). For presentation, all Photoshop manipulations (brightness and contrast only) were carried out equally across sections.

For double-label studies, sections were incubated overnight in a mixture of anti-Dab1 antibody (1:1,000) and one of the other antibodies listed in Table 1. Incubation with these antibodies used 0.5% Triton X-100 in 0.1 M PBS at 4°C. Sections were then rinsed for 30 minutes with 0.1 M PBS. Afterward, we incubated them with fluorescein isothiocyanate (FITC)-conjugated affinity-purified donkey anti-mouse IgG or donkey anti-goat IgG (1:100 dilution; Jackson Immunoresearch) or with Cy3-conjugated donkey anti-rabbit IgG (1:100 dilution; Jackson Immunoresearch) for 1–2 hours at room temperature. Sections were then washed again for 30 minutes with 0.1 M PB and coverslipped with 10% glycerol in 0.1 M PB. We also performed a control with these sections to confirm that the secondary antibody did not cross-react with an inappropriate primary antibody. Some sections were incubated in rabbit and goat polyclonal primary antibody followed by anti-mouse secondary antibody. Other sections were incubated in mouse primary antibody, followed by anti-rabbit secondary antibody. These sections showed no immunostaining.

Confocal laser scanning microscopy

Sections were analyzed by using a Bio-Rad Radiance Plus (Bio-Rad, Hemel Hempstead, United Kingdom) confocal scanning microscope, installed on a Nikon Eclipse E600 fluorescence microscope (Nikon, Tokyo, Japan). FITC and Cy3 fluorescence signals were always detected separately. FITC labeling was excited by using the 488-nm line of an argon ion laser and detected after passing an HQ513/30 (Bio-Rad) emission filter. For detection of the Cy3 signal, the 543-nm line of a green HeNe laser was used in combination with the 605/32 (Bio-Rad) emission filter. FITC and Cy3 images were imported into Adobe Photoshop 7.0. For presentation, all Photoshop manipulations (brightness and contrast only) were carried out equally across sections.

Topography and quantification

The topography of the distal Dab1-immunoreactive cell populations was analyzed in well-stained P7, P10, P21, and adult retinas. The cells were plotted using conventional microscopy. For quantifications of the number of cells, we obtained data from P5, P7, P10, P15, P21, and adult retinas. We used Pearson's correlation coefficient to analyze the similarity of this number in left vs. right eyes (four animals per stage). In turn, we used a one-way ANOVA to test the effect of age and litter on the number of cells. For the study of age, we focused on the left eye, sampling retinas from different litters, with 5 degrees of freedom (D.F.) between groups (six age groups) and 20 D.F. within groups (five retinas per age). The study of litters was performed separately at three ages, P7, P15, and P21. For each age, we had 2 D.F. between groups (three litters) and 6 D.F. within groups (three retinas per age).

Electron microscopy

For electron microscopy, three adult mice were euthanized as described above. Their eyecups were fixed in a mixture of 4% paraformaldehyde and 0.2% picric acid in PB for 30 minutes at room temperature. The retinas were then carefully dissected out; small pieces were taken from the central region and fixed for an additional 2 hours at 4°C. After being washed in PB, the pieces were transferred to 30% sucrose in PB for 6 hours at 4°C, rapidly frozen in liquid nitrogen, thawed, and embedded in 4% agar in distilled water. The retinal pieces were sectioned at 50 μm with a vibratome, and the sections were placed in PBS. They were incubated in 10% NGS in PBS for 1 hour at room temperature to block nonspecific binding and then in Dab1 antibody diluted 1:1,000 for 12 hours at 4°C.

The following immunocytochemical procedures for electron microscopy were carried out at room temperature. The sections were washed in PBS for 45 minutes (3 × 15 minutes), incubated in biotin-labeled goat anti-rabbit IgG for 2 hours, and then washed three times in PBS for 45 minutes (3 × 15 minutes). The sections were incubated in avidin-biotin-peroxidase complex (Vector Labaratories, Burlingame, CA; diluted to 1:100) for 1 hour, washed in TB, and then incubated in 0.05% 3,3′-diaminobenzidine (DAB) solution containing 0.01% H_2O_2. The reaction was monitored by using a low-power microscope and was stopped by replacing the DAB-H_2O_2 solution with TB.

The stained sections were postfixed in 1% glutaraldehyde in PB for 1 hour, and, after washing in PB containing 4.5% sucrose for 15 minutes (3 × 5 minutes), sections were postfixed in 1% OsO_4 in PB for 1 hour. They were then washed again in PB containing 4.5% sucrose and dehydrated in a graded series of alcohol. During dehydration, they were stained en bloc with 1% uranyl acetate in 70% alcohol for 1 hour, infiltrated with propylene oxide, and flat embedded in Epon 812. After sections had been cured at 60°C for 3 days, well-stained areas were cut out and attached to an Epon support for further ultrathin sectioning with a Reichert-Jung ultratome. Ultrathin sections (70–90 nm thick) were collected on one-hole grids coated with Formvar and examined via transmission electron microscopy (Jeol 1200EX; Jeol, Tokyo, Japan).

RESULTS

Dab1 immunoreactivity in the mouse retina

Figure 1A and B show, respectively, low and high magnifications of vertical sections of a retina processed for Dab1 immunoreactivity. The somata of Dab1-immunoreactive cells were strongly immunostained and found mostly in the INL adjacent to the IPL border. These amacrine cells typically have a single primary dendrite that descends into the IPL. This dendrite then gives off several side branches, which run toward stratum 5 near the ganglion cell layer. In sublamina a, short immunoreactive dendritic processes with large, irregular endings originate from the primary process. These processes resemble the lobular appendages previously described for AII amacrine cells of rabbit, cat, rat, monkey, mouse, and guinea pig retinas (Famiglietti and Kolb, 1975; Vaney, 1985; Dacheux and Raviola, 1986; Wong et al., 1986; Mills and Massey, 1991; Young and Vaney, 1990; Vaney et al., 1991; Strettoi et al., 1992; Wässle et al., 1993, 1995; Rice and Curran, 2000; Lee et al., 2003, 2004).

At higher magnifications, one sees a distinct type of Dab1-immunoreactive cell. It is in the outer part of the INL adjacent to the OPL (Fig. 1C,D). The ascending dendrites of this cell run horizontally along the OPL of the mouse retina. Therefore, in this study, in addition to AII amacrine cells, we observed a distinct type of Dab1-immunoreactive cell in the outer part of the INL.

Figure 2 shows a whole mount processed for Dab1 immunoreactivity in the mouse retina. When we focused near the IPL, numerous Dab1-immunoreactive amacrine cell somata were distributed throughout the retina, and the lobules were visible in sublamina a of the IPL (Fig. 2A). In sublamina a, thin and short immunoreactive processes that had large, irregular endings originated from both the cell body and primary dendrite. These processes resembled the lobular appendages previously described for AII amacrine cells of the mammalian retina (Dacheux and Raviola, 1986; Mills and Massey, 1991; Vaney et al., 1991; Strettoi et al., 1992). The focal series shown in Figure 2B–D shows Dab1-immunoreactive cells at the outer part of the INL. Similar to normally placed AII cells, distal Dab1-immunoreactive cells had narrow dendritic fields, with many varicosities. Dendrites were encircled by distinctive lobular appendages that connected to the cell through thin processes. These processes usually arose from either the soma or the primary dendrite as in the normal AII cells. Figure 2E and F were taken from the same retinal field as Figures 2B–D but with higher magnification. Varicosities were visible, and they varied between 1 and 4 μm in diameter. Therefore, Dab1-immunoreactive cells in the outer part of the INL seem to

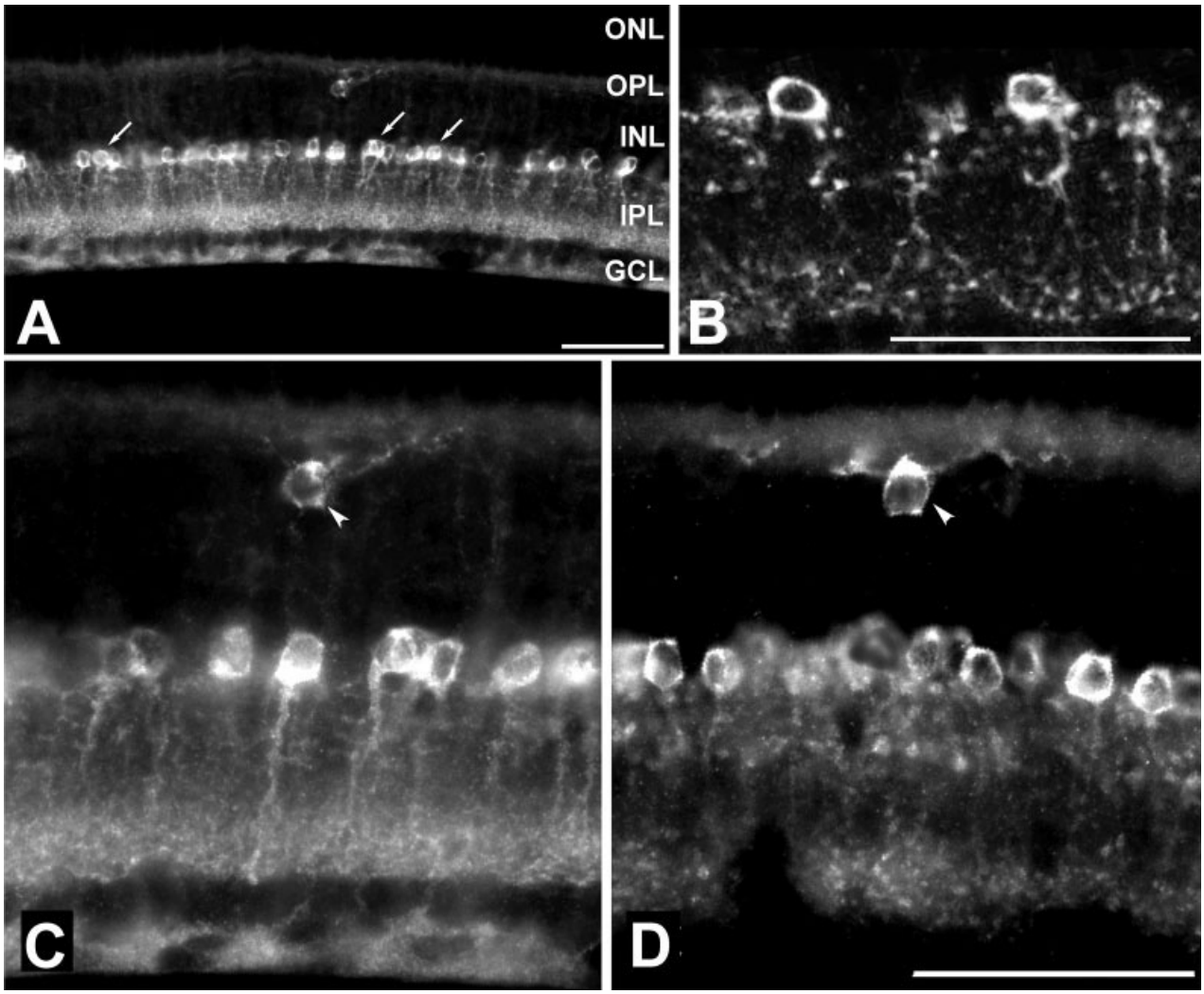

Fig. 1. Light micrographs of vertical sections of the C57BL/6J mouse retina processed for Dab1 immunoreactivity. **A:** Dab1 immunoreactivity is present on amacrine cell bodies (arrows) at the proximal INL and processes throughout the IPL. **B:** Higher power microphotographs of vertical sections of the C57BL/6J mouse retina processed for Dab1 immunoreactivity. Amacrine cells with lobular appendages and narrow dendritic fields are visible. **C,D:** Numerous Dab1-immunoreactive cells are visible in the proximal INL, but a different type of Dab1-immunoreactive cell appears in C and D (arrowheads). It is found in the outer part of the INL and has dendrites running horizontally along the OPL. ONL, outer nuclear layer; OPL, outer plexiform layer; INL, inner nuclear layer; IPL, inner plexiform layer; GCL, ganglion cell layer. Scale bars = 50 μm in A,B; 50 μm in D (applies to C,D).

have a morphology similar to that of Dab1-immunoreactive cells close to the IPL.

Double immunofluorescence for Dab1 with calbindin or Glyt-1

We tested whether the Dab1-immunoreactive cells in the outer part of the INL were horizontal cells. For this purpose, we performed double-labeling experiments with antisera against Dab1 and calbindin. Calbindin is a specific marker for horizontal cells in the mouse retina (Haverkamp and Wässle 2000). Figure 3 shows vibratome sections doubly labeled with antisera against Dab1 (Fig. 3A) and calbindin (Fig. 3B). In a merged image (Fig. 3C), Dab1-immunoreactive cells in the distal INL show no calbindin immunoreactivity. This strongly suggests that the Dab1-immunoreactive cells in the distal INL are not horizontal cells but a different type of neuron.

In the mammalian retina, most amacrine cells contain either glycine or γ-aminobutyric acid (GABA; Marc, 1989; Vaney, 1990; Marc et al., 1995; Vardi and Auerbach, 1995). Moreover, the Dab1 is known to label AII amacrine cells in the mammalian retina (Rice and Curran, 2000; Lee et al., 2003, 2004), which are glycinergic (Marc and Liu, 1984; Pourcho and Goebel, 1985; Grünert and Wässle, 1993; Goebel and Pourcho, 1997; Wright et al., 1997; Menger et al., 1998; Rice and Curran, 2000). Therefore, we performed double labeling with antisera against Dab1 and glycine transporter-1 (Glyt-1). Glyt-1 is a specific marker for glycinergic amacrine cells in the mouse retina (Haverkamp and Wässle, 2000). Figure 3D–F shows vibratome sections doubly labeled with antibodies against Dab1 (Fig. 3D) and Glyt-1 (Fig. 3E) in the mouse retina. All Dab1-immunoreactive amacrine cells in the INL adjacent to IPL and Dab1-immunoreactive cells in the distal INL showed

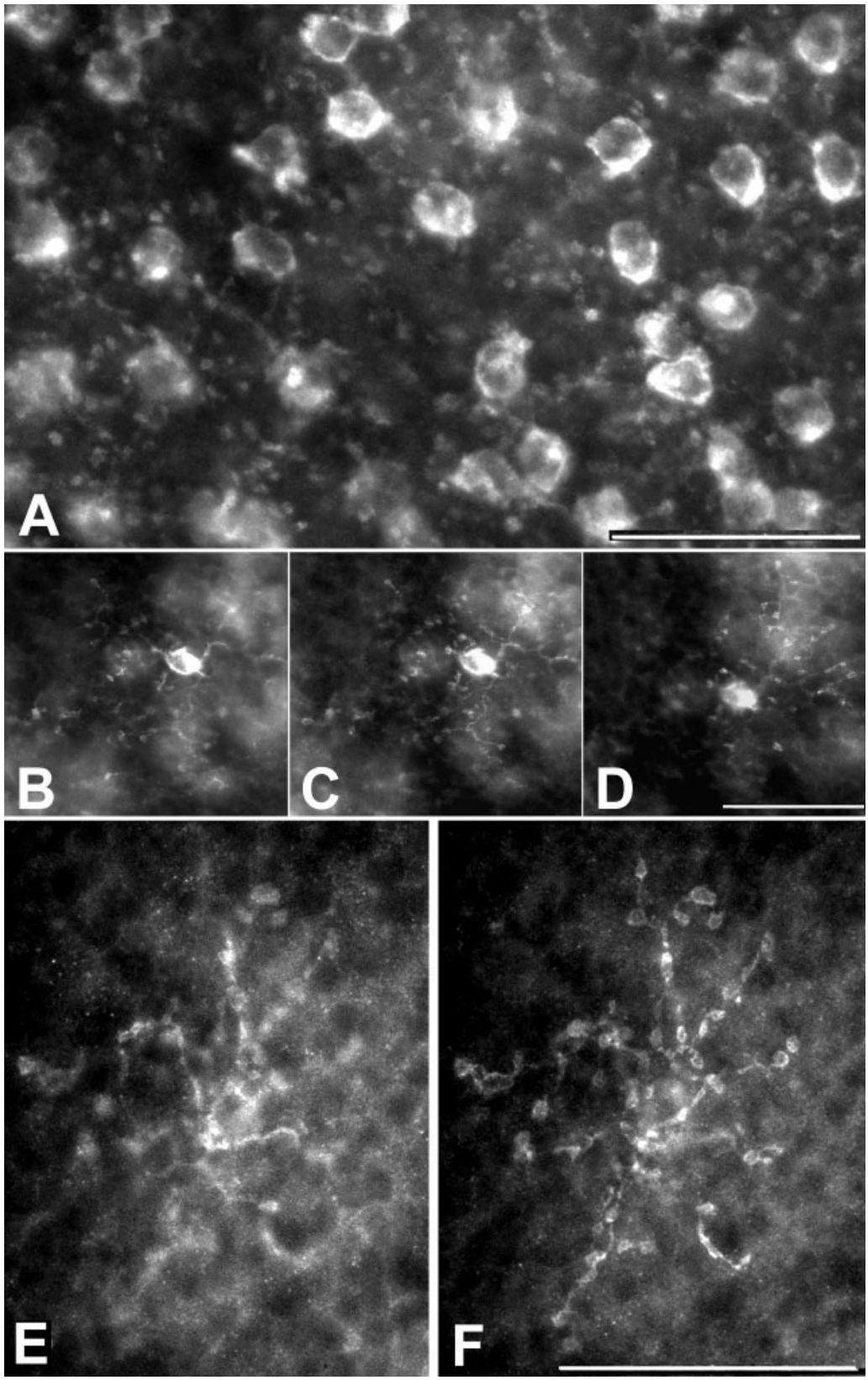

Fig. 2. Light micrographs taken at different focal planes in the same field of a whole-mount retina processed for Dab1 immunoreactivity. **A:** When the focus is on the IPL close to the INL, numerous Dab1-labeled amacrine cell bodies are visible. The numerous small dots are lobular appendages. **B–D:** The focal series of Dab1-immunoreactive cell at the outer part of the INL. Dab1-immunoreactive cells with a narrow dendritic field and many varicosities are visible. **E,F:** Higher power microphotographs of the same retinal field as B–D. Scale bars = 50 μm in A,D (applies to B–D); 50 μm in F (applies to E,F).

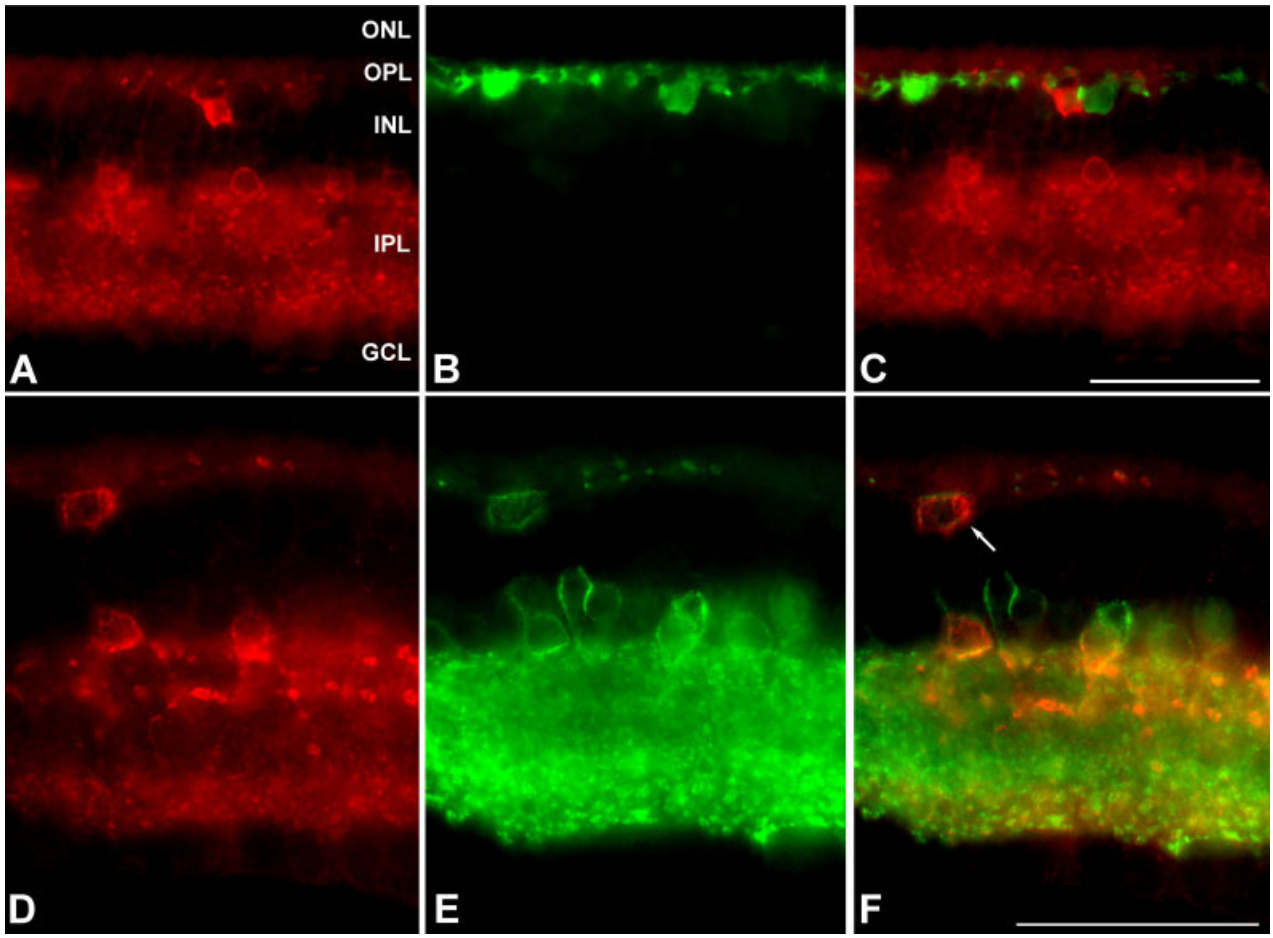

Fig. 3. Confocal micrographs of a vertical retinal section processed for Dab1 (**A**) and calbindin (**B**) immunoreactivity. Double exposure (**C**) shows no colocalization of Dab1 and calbindin in the outer part of the INL. D–F: Confocal micrographs of vertical retinal sections processed for Dab1 (**D**) and glycine transporter-1 (**E**) immunoreactivity. Double exposure (**F**) shows colocalization (yellow) of Dab1 and glycine transporter-1 in the outer part of the INL (arrow). Scale bars = 50 μm in C (applies to A–C), F (applies to D–F).

Glyt-1 immunoreactivity (Fig. 3F). In addition, these neurons did not show glutamic acid decarboxylase immunoreactivity (data not shown). Therefore, Dab1-immunoreactive cells in the outer part of the INL might use glycine as their neurotransmitter.

Dab1 immunoreactivity in the developing mouse retina and quantifications

The development of AII amacrine cells has been studied in the mammalian retina (Guo et al., 1992; Uesugi et al., 1992; Casini et al., 1998; Rice and Curran, 2000). Dab1 expression in the neural retina during the first week of postnatal development has also been reported (Rice and Curran, 2000). Here, we investigated whether there are Dab1-immunoreactive cells in the outer part of the INL from early developmental stages. At P3, Dab1 immunoreactivity was seen in radially oriented cells in the middle of neuroblastic layer (NBL). We also observed Dab1 cells in the proximal row of the NBL. These cells sent several immunoreactive branches into the presumptive IPL (Fig. 4A). At P5, most Dab1-immunoreactive cells were arranged in a single layer in the proximal row of the NBL and possessed many immunoreactive branches in the IPL (Fig. 4B). At the same time, a distinct type of Dab1-immunoreactive cell became apparent in the distal row of the NBL, where the presumptive OPL was forming (Fig. 4B). At P7, the dendrites of the new type of Dab1-immunoreactive cell run horizontally along the INL-OPL border, as shown in Figure 4C. From P7 onward, the new Dab1 cell was mature, showing a similar pattern as a function of age (Fig. 4D–F).

In whole-mount preparations, distal Dab1 cells appeared to have a random spatial distribution (Fig. 5). We could not perform a statistical test to ascertain this, because the number of cells was small, and retinal cuts often were between apparent near neighbors. However, near neighbors were either far apart (~1 mm) or very close (~50 μm), suggesting randomicity (Fig. 5). The large distance between most neighbors resulted in incomplete retinal coverage.

The number of these cells in the entire retina was never more than 40 per time point throughout development and into adulthood (Fig. 5). This number varied across animals, but the mean was statistically constant after P5

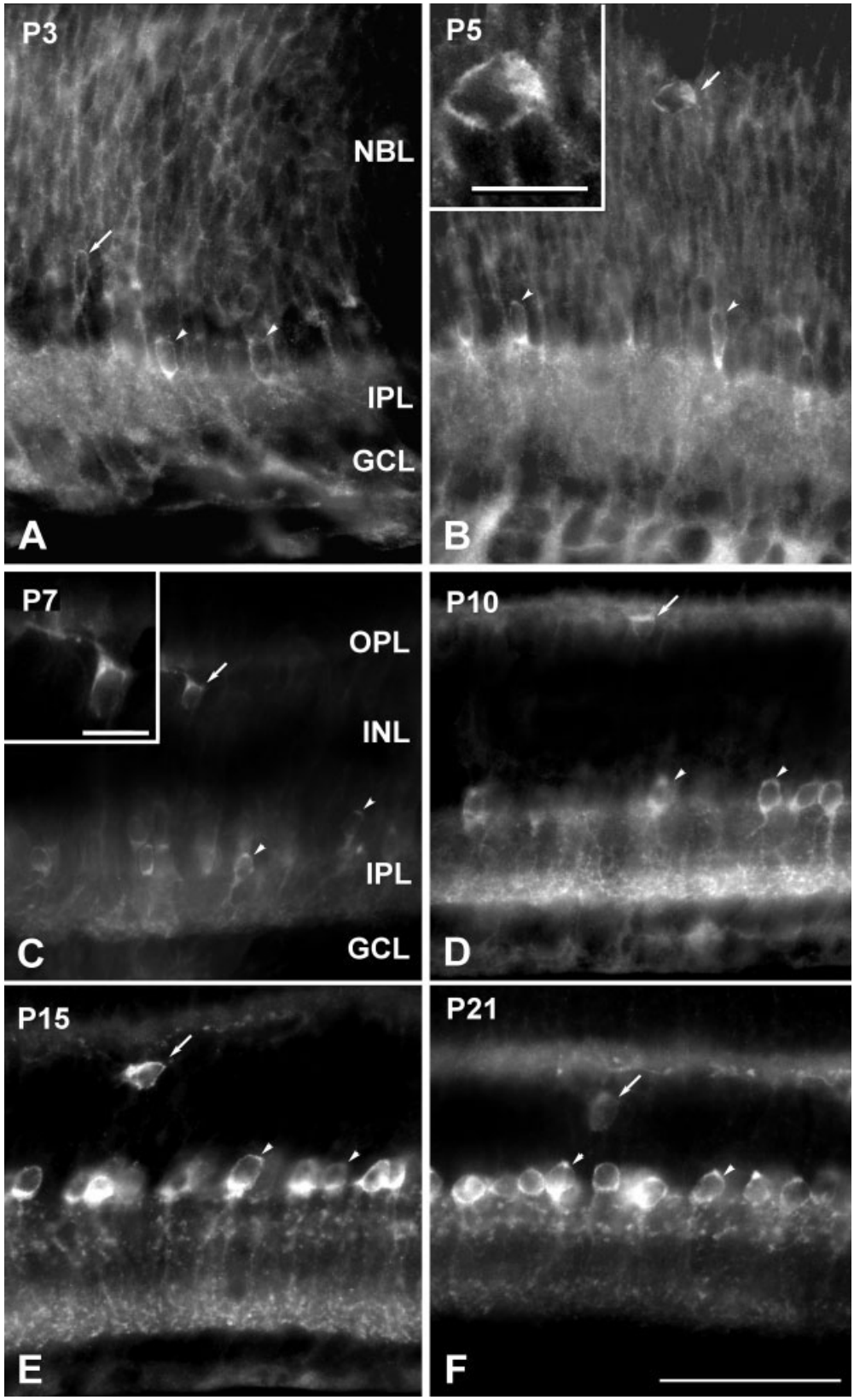

Fig. 4. Light microphotographs of developing mouse retinas processed for Dab1 immunocytochemistry. In P3 (**A**), Dab1 immunoreactivity is visible in radially oriented cells in the middle of NBL (arrow). Moreover, its proximal row contains Dab1 cells (arrowheads), extending several immunoreactive branches into the presumptive IPL. In P5 (**B**), Dab1 immunoreactivity shows in cells in the proximal row of the NBL (arrowheads). Its distal row also contains Dab1 cells (arrow). These cells are thus adjacent to where the presumptive OPL is going to form. In P7 (**C**), Dab1-immunoreactive cells (arrow) in the outer part of the INL show dendrites running horizontally along the INL-OPL border. In P10 (**D**), P15 (**E**), and P21 (**F**), Dab1-immunoreactive cells in the outer part of the INL show a pattern similar to that in P7 (C; arrows). The **insets** show higher magnification views of the cells marked by arrows. NBL, neuroblastic layer. Scale bars = 50 μm in F (applies to A–F); 10 μm in insets.

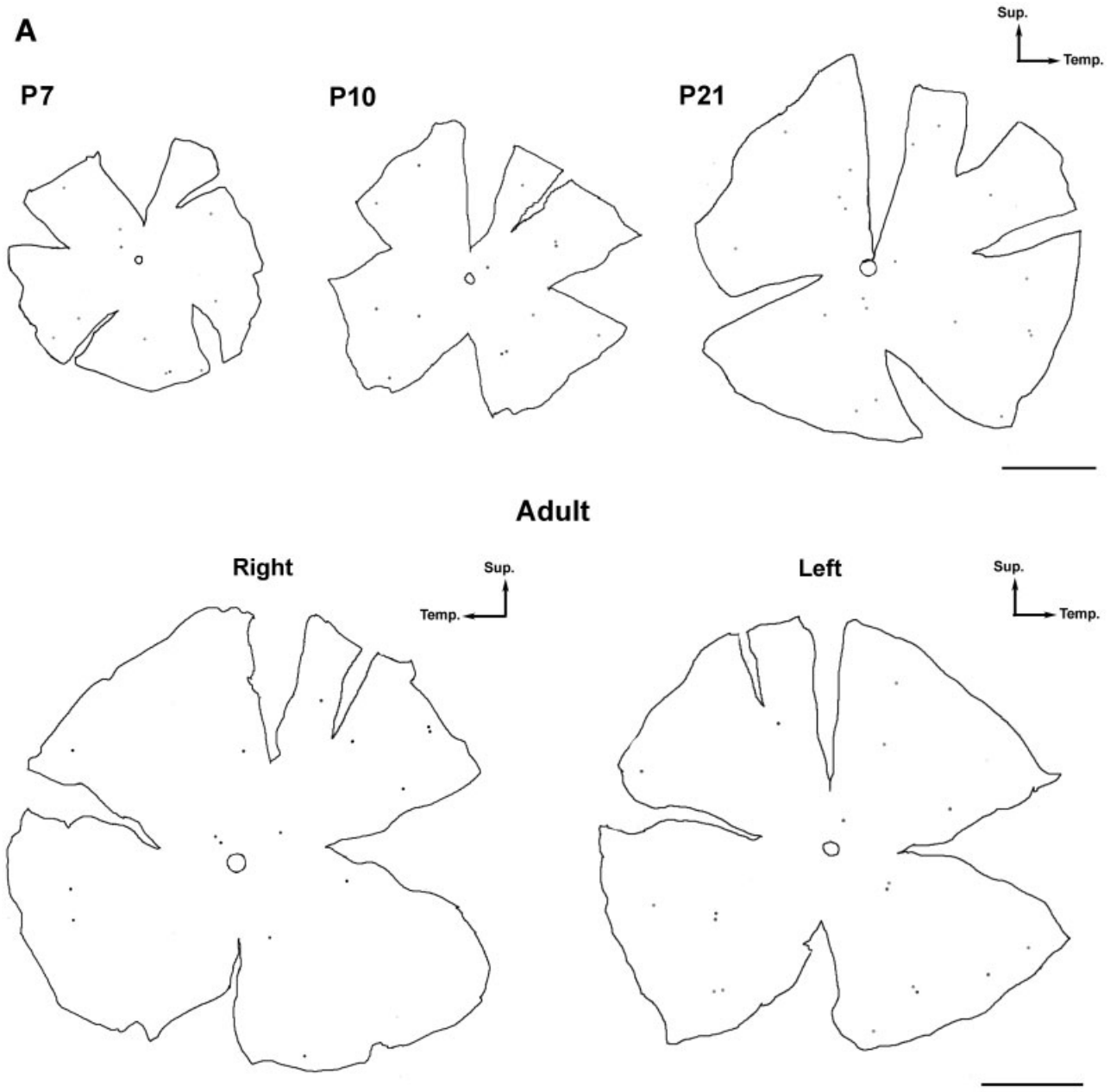

Fig. 5. Distribution of distal Dab1-immunoreactive cells in the outer part of the INL of P7, P10, P21, and adult whole-mounted retinas. Adult retinas are from left and right eyes of a single animal. P, postnatal; Sup, superior; Temp, temporal. Scale bars = 1 mm (applies to all).

(Fig. 6A; one-way ANOVA; Materials and Methods). The variation was such that the numbers of cells in the left and right eyes were similar (Fig. 5). This similarity yielded statistically significant correlation between the eyes (Fig. 6B; Pearson's correlation coefficient = 0.83, with lower and upper bounds for the 95% confidence interval = 0.64 and 0.92, respectively). This correlation suggested that the process determining the number of distal Dab1 cells was not entirely random. The correlation depended on a genetically controlled factor common to both eyes. To study this factor further, we also studied the effect of litter on the number of Dab1 cells. This number was not statistically significantly different across litters (one-way ANOVA; Materials and Methods).

Dab1 immunoreactivity in the outer plexiform layer

The long-term survival of a cell may depend on the establishment of functional connections (Rakic, 1975, 1988). Therefore, we examined the connections of distal Dab1-immunoreactive cell dendrites with other processes in the OPL of the adult retina. First, we tested whether

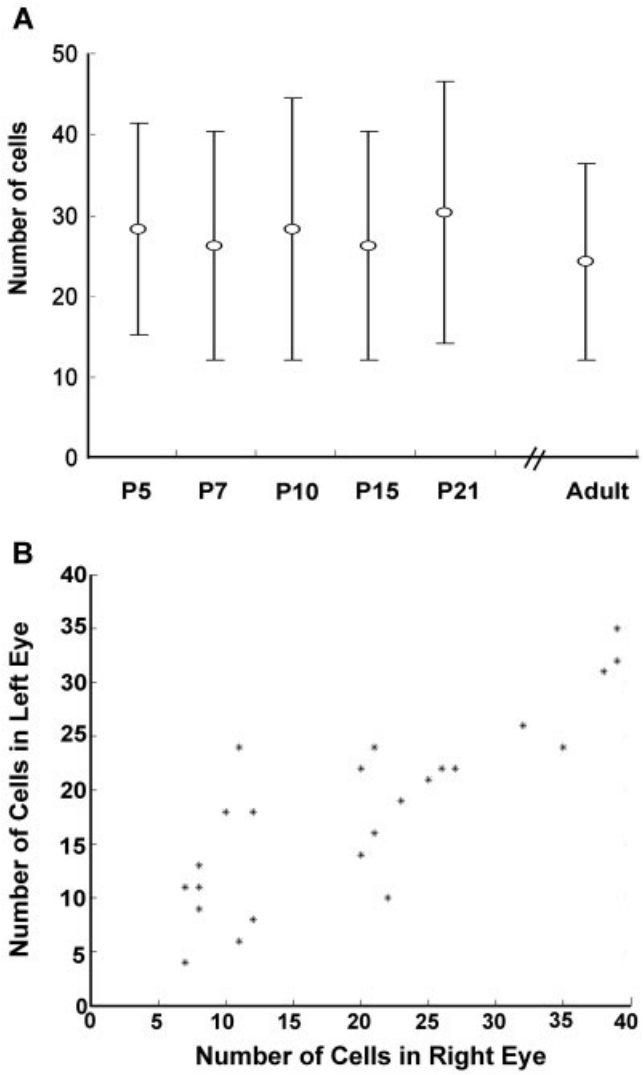

Fig. 6. Quantification of the number of distal Dab1 cells. **A:** Number of distal Dab1-immunoreactive cells in whole-mount retinas as a function of age. **B:** Correlogram of the numbers of distal Dab1-immunoreactive cells in left vs. right eyes (data mixing all available ages).

the Dab1-immunoreactive cell dendrites were making contact with horizontal cell dendrites. Figure 7A–C was taken from the same retinal field as Figure 4A–C but at higher magnification. In a merged image (Fig. 7C), Dab1-immunoreactive cell dendrites show close contact with horizontal cell dendrites. We also tested whether the Dab1-immunoreactive cell dendrites made close contact with photoreceptors or Glyt-1-immunoreactive interplexiform cells (Havercamp and Wässle, 2000). We performed double labeling with antisera against Dab1 and against Glyt-1 or against postsynaptic density (PSD-95), a specific marker for rods and cones in the mammalian retina (Koulen et al., 1998; Fletcher et al., 2000). Figure 7D–F shows vibratome sections doubly labeled with antibodies against Dab1 (Fig. 7D) and PSD-95 (Fig. 7E). Dendrites of Dab1-immunoreactive cells were separated from photoreceptor terminals (Fig. 7F). Figure 7G–I shows vibratome sections doubly labeled with antibodies against Dab1 (Fig. 7G) and Gly T-1 (Fig. H) in the mouse retina. Dendrites of Dab1-immunoreactive cells made close contacts with Glyt-1-immunoreactive processes. These results suggest that distal Dab1-immunoreactive cells are synaptically connected to horizontal cells, interplexiform cells, or both.

Synaptic ultrastructure of the distal Dab1-immunoreactive cell

The close contacts of the distal Dab1 cell described above are not enough to establish synaptic connectivity. To study synapses, we performed ultrastructural studies. These studies also helped us confirm that the distal Dab1-immunoreactive cells are the misplaced amacrine cells. Dab1 immunoreactivity produced an electron-dense reaction product that was closely associated with large mitochondrial membranes, cytoplasmic matrices, and synaptic vesicles (Fig. 8A,B). Amacrine synapses contain vesicles (Dubin, 1970; Kolb, 1979; McGuire et al., 1984), and AII amacrine cells have especially large mitochondria (Famiglietti and Kolb, 1975; Kolb, 1979; Chun et al., 1993). Furthermore, we observed synapses made onto Dab1-immunoreactive processes in the OPL. Figure 8 shows a labeled amacrine cell process receiving conventional synaptic input from an unlabelled interplexiform cell (Fig. 8A) and an unlabelled horizontal cell (Fig. 8B). However, in this study, we did not find Dab1-immunoreactive processes as presynaptic elements.

DISCUSSION

We describe a distal Dab1-immunoreactive, glycinergic cell in the retina of the mouse. It is unlikely that this cell was revealed by an artifact of processing or staining, because most amacrine cells labeled by antisera directed against Dab1 were in good agreement with previous reports on mammalian retinas (Rice and Curran, 2000; Lee et al., 2003, 2004). Moreover, the specificity of the Dab1 antibody is supported by previous studies using a Dab1 knockout mouse. Those studies showed no Dab1 immunostaining in the retina or in the brain (Rice and Curran, 2000; Hammond et al., 2001). The normal Dab1-labeled amacrine cells are located in a single row in the proximal INL. They have thick primary dendritic processes with branched lobular appendages in sublamina a of the IPL, and these processes ramify as bushy arbors in sublamina b. In contrast, the new distal Dab1-immunoreactive cells are in the outer part of the INL, adjacent to the OPL. Double labeling indicates that they are not horizontal cells. Rather, much of the microscopic and ultrastructural evidence presented herein suggests that distal Dab1 cells are misplaced amacrine cells. For instance, consider their dendrites, which run horizontally along the INL-OPL border. They define a narrow dendritic field with lobules similar to those found in AII amacrine cells. The varicosities in these dendrites vary between 1 and 4 μm in diameter. These diameters are consistent with lobular appendages of AII amacrine cells found in a previous study (Mills and Massey, 1999). However, although distal Dab1-immunoreactive cells are similar to AII amacrine cells in many respects, we encountered one difference. The distal neuron does not show bushy arbors like those of AII cells in the sublamina b of the IPL. This may be due to the narrowness of the OPL or the lack of trophic local factors in the OPL.

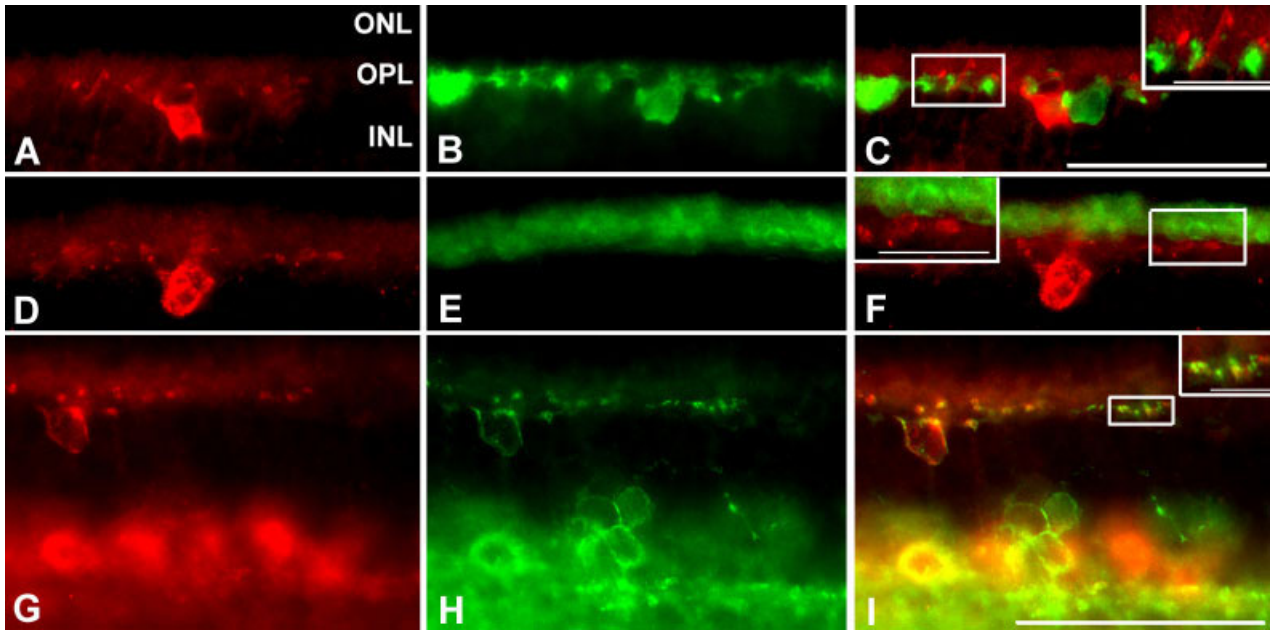

Fig. 7. Confocal micrographs of a vertical retinal section processed for Dab1 (**A**) and calbindin (**B**) immunoreactivities. Double exposure (**C**) shows close contact of Dab1- and calbindin-immunoreactive processes in the OPL. D–F: Confocal micrographs of vertical retinal sections processed for Dab1 (**D**) and PSD-95 (**E**) immunoreactivities. Double exposure (**F**) shows that processes of Dab1-immunoreactive cells in the OPL are apart from photoreceptor terminals. G–I: Confocal micrographs of vertical retinal sections processed for Dab1 (**G**) and glycine transporter-1 (**H**) immunoreactivity. Double exposure (**I**) shows colocalization (yellow) of Dab1 and glycine transporter-1 in the outer part of the INL. Scale bars = 50 μm in C (applies to A–F); 50 μm in I (applies to G–I); 10 μm in insets.

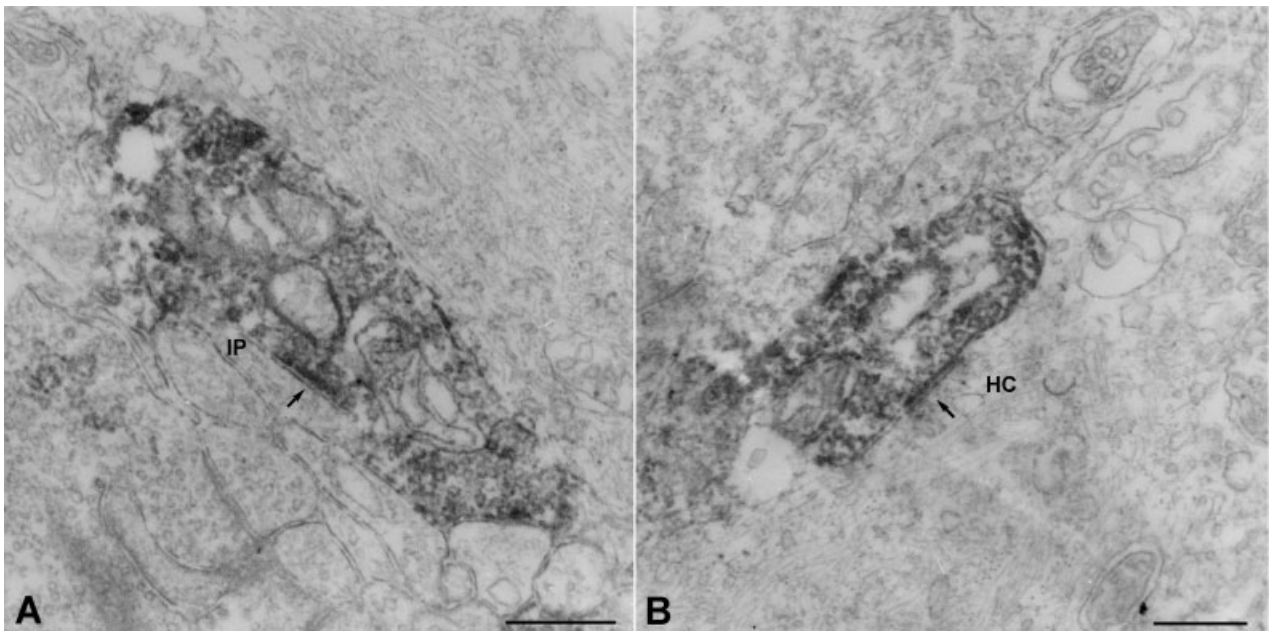

Fig. 8. Electron micrograph taken from a vertical ultrathin section of the OPL of a mouse retina processed for Dab1 immunoreactivity. **A:** A labeled amacrine cell process receives synaptic input (arrow) from an unlabeled interplexiform cell process in the OPL. **B:** A labeled amacrine cell process receives synaptic input (arrow) from an unlabeled horizontal cell process in the OPL. IP, interplexiform cell; HC, horizontal cell. Scale bars = 0.2 μm.

Distal Dab1 cells have been reported in the FVB/N mouse retina (Park et al., 2004). That retina is a model of retinitis pigmentosa. Consequently, the authors who described distal Dab1 cells in that retina suggest that their ascending processes in the OPL are due to loss of photoreceptors during development (Park et al., 2004). This interpretation was supported by the authors' failure to find distal Dab1-immunoreactive cells in the control retinas. In contrast, we found such cells in both the C57BL/6J and the BALB/C (data not shown) mouse retinas. Although this type of cell was rare, it was consistently found in both strains of mouse and in all stages of postnatal development. Therefore, the appearance of these cells might not necessitate the loss of photoreceptors. However, the number of distal Dab1-immunoreactive cells seems to be higher in the FVB/N mouse (53 ± 18; Park et al., 2004) than in our species (26 ± 14). This suggests that losing photoreceptors might increase the number of distal Dab1-immunoreactive cells in the retina. Another factor that may control the number of distal Dab1 cells is genetic. If this number were entirely randomly determined, then one would not expect a correlation between the eyes. We found such a correlation, suggesting that the eyes have a common factor controlling the number. We suggest that this factor is genetically determined. However, if this is the case, then the factor must involve several competing alleles, insofar as different animals from a litter may have different numbers of Dab1 distal cells.

Haverkamp and Wässle (2000) and Kang et al. (2004) have shown that there are GABA- and ChAT-immunoreactive cells, respectively, in the outer part of the INL. They have interpreted them as "misplaced" amacrine cells. In addition, misplaced cells have been reported in different mammalian species (Nelson, 1982; Vaney, 1985, 1990; Sandell and Masland, 1989; Silveira et al., 1989; Peichl and Gonzales-Soriano, 1994; Wässle et al., 2000; Eglen et al., 2003). Therefore, a distal Dab1, glycinergic immunoreactive cell in the distal INL reinforces the idea that "misplaced" amacrine cells may be a common feature of normal retinas of many species. It is conceivable that all, or most, kinds of amacrine cells have elements displaced to the outer INL or other nuclear layers. This conclusion may hold regardless of neurotransmitter.

We suggest that these various kinds of misplaced amacrine cells represent developmental errors rather than being neurons with significant visual functions. One reason for this suggestion is that these cells are sparse, defining coverage factors much lower than one. Hence, if their neurotransmitters were to have an effect on the outer retina, they would have a spatially nonhomogeneous action. Alternatively, these cells would have to operate by slow diffusion, being very slow. Another reason for suspecting that misplaced amacrine cells are "errors" is that these neurons do not form regular mosaics (for review see Sterling, 1983). W¨assle and Riemann (1978) have suggested that somata arranged in regular mosaics are a hallmark of homogeneous, functional retinal populations.

We thus investigated whether these "misplaced" AII amacrine cells are present from early developmental stages. Our goal was to see whether we could detect any evidence of developmental errors. At P3, we could visualize some Dab1-immunoreactive profiles migrating in the NBL and some Dab1-immunoreactive cells located close to the IPL. The latter cells extended their neurites into the inner retina. At P5, most Dab1-immunoreactive cells were arranged in a single layer in the proximal row of the NBL. They possessed many immunoreactive branches in the IPL. However, at the same time, one could already see the new distal Dab1-immunoreactive cells in the distal row of the NBL. Given our arguments that these cells are developmental errors, we suggest that these cells were mistakenly omitted. The presence of these neurons outside their normal location of the NBL (i.e., proximal row of the NBL) might reflect migration errors during early development. A possible explanation for this sequence of events is that these cells were the last ones to start migrating, and the space available for migration closed up before they finished their travel. Alternatively, these cells perhaps failed to recognize a signal to keep migrating when they were in the middle of the NBL. This signal may be reelin. Reelin is expressed in three different retinal cell types, including ganglion cells, amacrine cells, and cone bipolar cells (Rice et al., 2001). Failure to receive a reelin-induced signal from one or more of these sources might lead to the alteration in the distribution of the AII cell (Rice and Curran, 2000). Dab1 is a critical component of the reelin signaling pathway that controls laminar organization in the brain (see the introductory paragraphs).

The number of distal Dab1-immunoreactive cells in the outer part of the INL is constant from P5 to adulthood. The long-term survival of such a cell may depend on the establishment of functional connections (Rakic, 1975, 1988). We used electron microscopy to study the synaptic connectivity of Dab1-immunoreactive cells in the OPL. These misplaced cells receive connections with glycinergic interplexiform cells and horizontal cells in the OPL. Although glycine-accumulating interplexiform cell in vertebrate retina normally make synapses with horizontal cells (Marc and Liu, 1984), our findings suggest that these are not the only synapses from this cell. The evidence for such contacts is supported by the punctate glycine receptor in the OPL (Vitanova et al., 2004). Therefore, distal Dab1-immunoreactive cell may have glycinergic receptors. Furthermore, this cell receives synaptic input from horizontal cells. This result seems odd, because horizontal cells are known to contact only photoreceptors and bipolar cells (Dowling et al., 1966; Limberg and Fisher, 1988). In any event, we do not know what role this misplaced AII cell plays in the OPL. Whether such functional contacts play a role in the processing of visual information remains to be established.

It is interesting that the new distal Dab1-immunoreactive cell sends dendrites into the OPL. If this cell normally sends dendrites into the IPL, then it is not a priori obvious that the cell has the receptors to recognize OPL neurotrophic factors. Our data suggest that it does. This raises the possibilities that the OPL and IPL use similar neurotrophic factors and that different INL cells express similar kinds of neurotrophic receptors.

ACKNOWLEDGMENTS

We thank Hong-Lim Kim for technical assistance; David Merwine, Mónica Padilla, Joaquín Rapela, Jeff Wurfel, and Susmita Chatterjee for discussions during this work; and Denise Steiner for administrative support.

LITERATURE CITED

Casini G, Rickman DW, Trasarti L, Brecha NC. 1998. Postnatal development of parvalbumin immunoreactive amacrine cells in the rabbit retina. Brain Res Dev Brain Res 111:107–117.

Chun MH, Han SH, Chung JW, Wässle H. 1993. Electron microscopic analysis of the rod pathway of the rat retina. J Comp Neurol 332:421–432.

Dacheux RF, Raviola E. 1986. The rod pathway in the rabbit retina: a depolarizing bipolar and amacrine cell. J Neurosci 6:331–345.

Dowling JE, Brown JE, Major D. 1966. Synapses of horizontal cells in rabbit and cat retinas. Science 153:1639–1641.

Dubin MW. 1970. The inner plexiform layer of the vertebrate retina: a quantitative and comparative electron microscopic analysis. J Comp Neurol 140:479–505.

Eglen SJ, Raven MA, Tamrazian E, Reese BE. 2003. Dopaminergic amacrine cells in the inner nuclear layer and ganglion cell layer comprise a single functional retinal mosaic. J Comp Neurol 466:343–355.

Famiglietti EV Jr, Kolb H. 1975. A bistratified amacrine cell and synaptic circuitry in the inner plexiform layer of the retina. Brain Res 84:293–300.

Fletcher EL, Hack I, Brandstatter JH, Wässle H. 2000. Synaptic localization of NMDA receptor subunits in the rat retina. J Comp Neurol 420:98–112.

Goebel DJ, Pourcho RG. 1997. Calretinin in the cat retina: colocalizations with other calcium-binding proteins, GABA and glycine. Vis Neurosci 14:311–322.

Grzywacz NM, Lee EJ, Mann LB, Rickman DW. 2005. Ectopic AII amacrine cells in the developing and adult mouse retinas. Invest Ophthalmol Vis Sci 46 (E-abstract 585).

Guo QX, Yu MC, Garey LJ, Jen LS. 1992. Development of parvalbumin immunoreactive neurons in normal and intracranially transplanted retinas in the rat. Exp Brain Res 90:359–368.

Hammond V, Howell B, Godinho L, Tan SS. 2001. Disabled-1 functions cell autonomously during radial migration and cortical layering of pyramidal neurons. J Neurosci 21:8798–8808.

Haverkamp S, Wässle H. 2000. Immunocytochemical analysis of the mouse retina. J Comp Neurol 424:1–23.

Howell BW, Gertler FB, Cooper JA. 1997. Mouse disabled (mDab1): an Src binding protein implicated in neuronal development. EMBO J 16:121–132.

Kang TH, Ryu YH, Kim IB, Oh GT, Chun MH. 2004. Comparative study of cholinergic cells in retinas of various mouse strains. Cell Tissue Res 317:109–115.

Kolb H. 1979. The inner plexiform layer in the retina of the cat: electron microscopic observations. J Neurocytol 8:295–329.

Kolb H, Famiglietti EV. 1974. Rod and cone pathways in the inner plexiform layer of cat retina. Science 186:47–49.

Koulen P, Fletcher EL, Craven SE, Bredt DS, Wässle H. 1998. Immunocytochemical localization of the postsynaptic density protein PSD-95 in the mammalian retina. J Neurosci 18:10136–10149.

Lee EJ, Kim HJ, Kim IB, Park JH, Oh SJ, Rickman DW, Chun MH. 2003. Morphological analysis of Disabled-1-immunoreactive amacrine cells in the guinea pig retina. J Comp Neurol 466:240–250.

Lee EJ, Kim HJ, Lim EJ, Kim IB, Kang WS, Oh SJ, Rickman DW, Chung JW, Chun MH. 2004. AII amacrine cells in the mammalian retina show disabled-1 immunoreactivity. J Comp Neurol 470:372–381.

Linberg KA, Fisher SK. 1988. Ultrastructural evidence that horizontal cell axon terminals are presynaptic in the human retina. J Comp Neurol 268:281–297.

Marc RE. 1989. The role of glycine in the mammalian retina. Prog Ret Res 8:67–107.

Marc RE, Liu WL. 1984. (^{3}H)glycine-accumulating neurons of the human retina. J Comp Neurol 232:241–260.

Marc RE, Murry RF, Basinger SF. 1995. Pattern recognition of amino acid signatures in retinal neurons. J Neurosci 15:5106–5129.

Margolis B. 1996. The PI/PTB domain: a new protein interaction domain involved in growth factor receptor signaling. J Lab Clin Med 128:235–241.

McGuire GA, Stevens JK, Sterling P. 1984. Microcircuitry of bipolar cells in cat retina. J Neurosci 4:2920–2938.

Menger N, Pow DV, Wässle H. 1998. Glycinergic amacrine cells of the rat retina. J Comp Neurol 401:34–46.

Mills SL, Massey SC. 1991. Labeling and distribution of AII amacrine cells in the rabbit retina. J Comp Neurol 304:491–501.

Mills SL, Massey SC. 1999. AII amacrine cells limit scotopic acuity in central macaque retina: a confocal analysis of calretinin labeling. J Comp Neurol 411:19–34.

Nelson R. 1982. AII amacrine cells quicken time course of rod signals in the cat retina. J Neurophysiol 47:928–947.

Park SJ, Lim EJ, Oh SJ, Chung JW, Rickman DW, Moon JI, Chun MH. 2004. Ectopic localization of putative AII amacrine cells in the outer plexiform layer of the developing FVB/N mouse retina. Cell Tissue Res 315:407–412.

Peichl L, Gonzalez-Soriano J. 1994. Morphological types of horizontal cell in rodent retinae: a comparison of rat, mouse, gerbil, and guinea pig. Vis Neurosci 11:501–517.

Pourcho RG, Goebel DJ. 1985. A combined Golgi and autoradiographic study of (^{3}H)glycine-accumulating amacrine cells in the cat retina. J Comp Neurol 233:473–480.

Rakic P. 1975. Cell migration and neuronal ectopias in the brain. Birth Defects Orig Art Ser 11:95–129.

Rakic P. 1988. Defects of neuronal migration and the pathogenesis of cortical malformations. Prog Brain Res 73:15–37.

Rice DS, Curran T. 1999. Mutant mice with scrambled brains: Understanding the signaling pathways that control cell positioning in the CNS. Genes Dev 13:2758–2773.

Rice DS, Curran T. 2000. Disabled-1 is expressed in type AII amacrine cells in the mouse retina. J Comp Neurol 424:327–338.

Rice DS, Nusinowitz S, Azimi AM, Martinez A, Soriano E, Curran T. 2001. The reelin pathway modulates the structure and function of retinal synaptic circuitry. Neuron 31:929–941.

Sandell JH, Masland RH. 1989. Shape and distribution of an unusual retinal neuron. J Comp Neurol 280:489–497.

Silveira LC, Yamada ES, Picanco-Diniz CW. 1989. Displaced horizontal cells and biplexiform horizontal cells in the mammalian retina. Vis Neurosci 3:483–488.

Sterling P. 1983. Microcircuitry of the cat retina. Annu Rev Neurosci 6:149–185.

Strettoi E, Dacheux RF. 1992. Synaptic connections of the narrow-field, bistratified rod amacrine cell (AII) in the rabbit retina. J Comp Neurol 325:152–168.

Uesugi R, Yamada M, Mizuguchi M, Baimbridge KG, Kim SU. 1992. Calbindin D-28k and parvalbumin immunohistochemistry in developing rat retina. Exp Eye Res 54:491–499.

Vaney DI. 1985. The morphology and topographic distribution of AII amacrine cells in the cat retina. Proc R Soc Lond B Biol Sci 224:475–488.

Vaney DI. 1990. The mosaic of amacrine cells in the mammalian retina. Prog Ret Res 9:49–100.

Vaney DI, Gynther IC, Young HM. 1991. Rod-signal interneurons in the rabbit retina: 2. AII amacrine cells. J Comp Neurol 310:154–169.

Vardi N, Auerbach P. 1995. Specific cell types in cat retina express different forms of glutamic acid decarboxylase. J Comp Neurol 351:374–384.

Vitanova L, Haverkamp S, Wässle H. 2004. Immunocytochemical localization of glycine and glycine receptors in the retina of the frog *Rana ridibunda*. Cell Tissue Res 317:227–235.

Wässle H, Riemann HJ. 1978. The mosaic of nerve cells in the mammalian retina. Proc R Soc Lond B Biol Sci 200:441–461.

Wässle H, Grünert U, Röhrenbeck J. 1993. Immunocytochemical staining of AII-amacrine cells in the rat retina with antibodies against parvalbumin. J Comp Neurol 332:407–420.

Wässle H, Grunert U, Chun MH, Boycott BB. 1995. The rod pathway of the macaque monkey retina: identification of AII-amacrine cells with antibodies against calretinin. J Comp Neurol 361:537–551.

Wässle H, Dacey DM, Haun T, Haverkamp S, Grunert U, Boycott BB. 2000. The mosaic of horizontal cells in the macaque monkey retina: with a comment on biplexiform ganglion cells. Vis Neurosci 17:591–608.

Wong ROL, Henry GH, Medveczky CJ. 1986. Bistratified amacrine cells in the retina of the Tammar wallaby, *Macropus eugenii*. Exp Brain Res 63:102–105.

Wright LL, Macqueen CL, Elston GN, Young HM, Pow DV, Vaney DI. 1997. DAPI-3 amacrine cells of the rabbit retina. Vis Neurosci 14:473–492.

Young HM, Vaney DI. 1990. The retinae of prototherian mammals possess neuronal types that are characteristic of non-mammalian retinae. Vis Neurosci 5:61–66.